Received: 2 March 2023 | Revised: 4 May 2023 | Accepted: 22 May 2023

DOI: 10.1111/ter.12667

RESEARCH ARTICLE

Terra Nova WILEY

Imaging of post-collisional deformations on the NE Tisza continental unit using ambient seismic noise: A case study from the Ţicău area, Romania

Ionelia Panea[1] | Deyan Draganov[2] | Catalin Florin Bouaru[1] | Ioan Munteanu[1]

[1]Faculty of Geology and Geophysics, University of Bucharest, Bucharest, Romania

[2]Faculty of Civil Engineering and Geosciences, Delft University of Technology, Delft, The Netherlands

Correspondence
Ionelia Panea, Faculty of Geology and Geophysics, University of Bucharest, Bucharest, Romania.
Email: ionelia.panea@gmail.com

Funding information
Norway Grants, UEFISCDI

Abstract

The Ţicău area (NW Romania) is part of the collisional zone between the Tisza and Dacia mega-units. Imaging of Ţicău area's subsurface geological structure will contribute to the understanding of the processes, which controlled its tectonic evolution. Analysis of outcrops provides accurate information for the building of kinematic sections used to explain the small-scale deformations of sedimentary formations, such as those developed south of the Ţicău mountains. Imaging of large-scale deformations requires analysis of data recorded and/or measured over a wider area. We use Seismic Interferometry by cross-correlation on ambient noise recorded along with a line located north of the Ţicău mountains. The passive seismic section obtained after virtual body-wave reflections processing displays folded and faulted Paleogene formations, which are in good agreement with the observations on outcrops found to the south of the Ţicău mountains. The active-source data recorded along with the same line are too noisy for interpretation.

KEYWORDS
ambient seismic noise, Interferometry, Tisza and Dacia mega-units

1 | INTRODUCTION

The present-day architecture of the sedimentary and metamorphic formations from the Ţicău area is resulted from the tectonic evolution of the Tisza and Dacia mega-units until the late Early Cretaceous and the formation and evolution of the Eastern Pannonian Basin during the Miocene to Quaternary times (Figure 1). Tectonic models at various scales have been proposed for the Eastern Pannonian Basin in order to explain the processes, which had taken place (e.g. Schmid et al., 2008). The building of these models is correlated with the evolution of the surrounding tectonic units, using information from surface geological mapping, geophysical measurements and radioactive dating of rock samples (e.g. Ciulavu et al., 2002; Merten et al., 2011; Răbăgia, 2009; Reiser et al., 2019; Săndulescu, 1988).

The Ţicău mountains, developed in the southern part of the area, are made of nappes belonging to the Tisza mega-unit. Towards north, these nappes are covered by Pre-Neogene and Neogene deposits. In the existent literature, the Ţicău mountains are also named the Ţicău uplift or the Ţicău crystalline island. Useful information about the post-collisional deformation of the pre-Neogene and Neogene sedimentary deposits developed south of the Ţicău mountains is provided by surface geological mapping of small outcrops and by the contractional, extensional and strike-slip data measured in the field (Merten et al., 2011). Obtaining of such information, though, depends on the presence of exposed outcrops in the study area. The outcrops help us identify and analyse the lithology and the ruptural (or not) deformations.

When outcrops are lacking, alternative investigation methods should be used, such as the seismic exploration method with active and/or passive sources. The active-source techniques are based on the use of controlled sources of seismic energy (e.g. explosives, vibrators). In the passive-source method, spreads of wireless or cable-connected receivers record the ambient seismic noise from natural and cultural uncontrolled sources, such as small earthquakes, movement of underground waters, surface traffic, industrial activity, etc. The recorded noise can be used directly to obtain P- and S-wave velocity-depth distributions in the subsurface or after a processing, which allow obtaining time and/or depth-converted seismic sections.

Seismic Interferometry (SI) by cross-correlation is a technique used to retrieve seismic responses between receivers using, for example ambient-noise recordings at the receivers. These retrieved responses are at least proportional to those generated by an active source at the location of one of the receiver and recorded at the other receiver. The retrieval of reflection responses with the SI method was first proposed by Claerbout (1968) for 1D media and later extended to a general 3D inhomogeneous medium using reciprocity theorems of the correlation and convolution type (van Manen et al., 2005; Wapenaar et al., 2002; Wapenaar & Fokkema, 2006). The method was applied for retrieval of surface waves using SI by cross-correlation for example from ambient noise generated by sources located near or at the Earth's surface (e.g. Sabra et al., 2005; Shapiro & Campillo, 2004). It was also used for the retrieval of body-wave reflections from ambient noise (e.g. Draganov et al., 2009; Hohl & Mateeva, 2006; Panea et al., 2014; Ruigrok et al., 2011; Xu et al., 2012; Zhan et al., 2010). Comparative analyses between retrieved reflections from ambient noise and reflections from active-source seismic reflection measurements showed good correspondences between them, especially at lower frequencies (e.g. Draganov et al., 2009; Panea et al., 2014).

Significance Statement

Geological mapping and measurements on outcrops provide accurate information about the tectonic processes in which the basement and its sedimentary cover can be involved. The obtaining of this information depends on the presence of outcrops, otherwise, methods of subsurface investigation, which are less dependent on outcrops must be used. In this paper, we report results of active- and passive-source seismic measurements performed for the first time in the Ţicău area, which is situated on the collisional zone between the Tisza and Dacia mega-units. The Ţicău mountains from this area belong to the row of crystalline islands, which separate the Pannonian and Transylvanian basins. The structural image of the post-collisional sedimentary cover obtained after interpretation of the passive seismic section helps us understand the tectonic evolution of this area. Our interpretation is in good agreement with the results of surface geological mapping and measurements performed only on outcrops found to south of our study area.

In the following, we use seismic measurements to study the subsurface structures in the Ţicău area. We use SI by cross-correlation to retrieve body-wave reflections from ambient-noise seismic data recorded along with a line. We do this because active-source seismic reflection measurements could not be properly performed in the area due to the field conditions. We process the retrieved reflections to obtain a seismic section, which provides an image of the subsurface geological structures of the pre-Neogene and Neogene deposits in our study area.

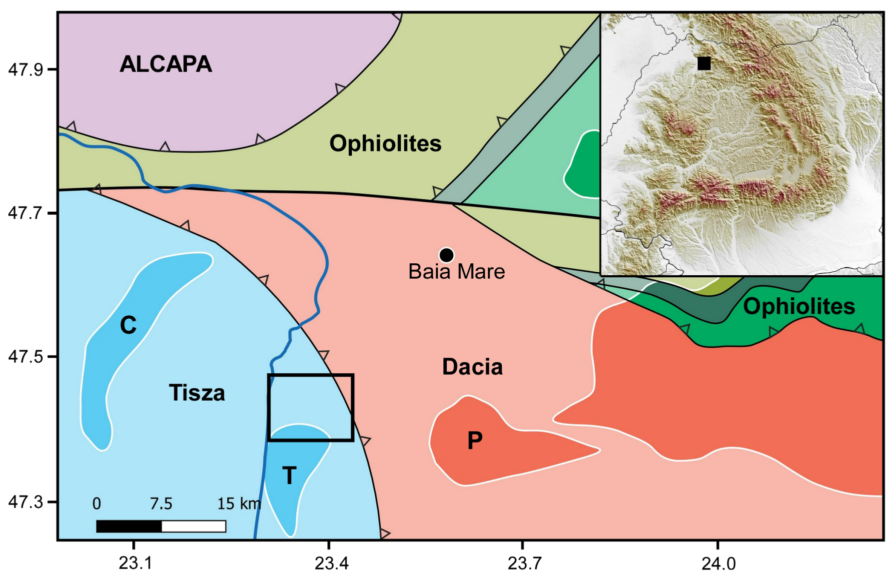

FIGURE 1 Tectonic map showing the contact between the Tisza and Dacia Mega-units in the NW Romania (edited crop from Schmid et al., 2020). T, P and C – Ţicău, Preluca and Codru crystalline islands. Inset – map of Romania showing the location of the study area (black rectangle). [Colour figure can be viewed at wileyonlinelibrary.com]

2 | GEOLOGICAL SETTING OF THE ŢICĂU AREA

The Ţicău area is situated on the north-eastern margin of the Eastern Pannonian Basin from the Romanian territory. Tectonically, it belongs to the collisional zone between the Tisza and Dacia mega-units (Figure 1). Dacia, developed towards east and south-east, was sutured to Tisza, from west, during the late Jurassic – late Early Cretaceous closure of the north-eastern branch of the Neotethys Ocean (e.g. Balázs et al., 2016; Săndulescu, 1988; Schmid et al., 2008). In the north-west, the ALCAPA (ALpine-CArpathian-PAnnonian) mega-unit was sutured to Europe during the northward closure of the Alpine Tethys from Cretaceous-Eocene (e.g. Csontos, 1995; Schmid et al., 2004). The ALCAPA and Tisza-Dacia mega-units were juxtaposed along with a major suture zone known as the Mid-Hungarian Fault Zone (MHFZ); their movements and rotations are correlated with the tectonic evolution of the Pannonian Basin and Alps-Carpathians (e.g. Balázs et al., 2016; Balla, 1987; Csontos, 1995; Horváth et al., 2015; Kalmár et al., 2021; Márton & Fodor, 2003; Săndulescu, 1988; Schmid et al., 2004). The prolongation of the MHFZ on the Romanian territory is known as the Bogdan-Dragos-Voda fault system (BDV in Figure 2).

The degree and type of post-collisional sedimentary deformations in the contact area between the Tisza and Dacia mega-units have been evaluated using information obtained from observations and measurements of existing outcrops. According to Merten et al. (2011), Miocene thrust and reverse faulting, Eocene E-W folding and Miocene NNW–SSE folding had affected the sedimentary formations of the Paleogene age located to the south of the Ţicău mountains.

For our study area, information about the subsurface geological structure is presented mainly from the surface mapping of three large outcrops found in the western part of the Ţicău mountains along with a national road connecting villages north and south of these mountains; their locations are indicated in Figure 2 (O_1, O_2 and O_3). From a lithological point of view, the basement is made up of metamorphic rocks of Precambrian-Palaeozoic ages, similar to what is currently exposed in the surrounding mountains (e.g. Ciulavu et al., 2002). The basement crops out in green-schist facies in the southwestern part of the Ţicău mountains (O_1 and O_2 in Figure 3). The metamorphic rocks are strongly deformed (folded and faulted) as a result of the collision between the Tisza and Dacia mega-units. Towards north, the basement is directly covered by Paleogene and Neogene sedimentary formations (e.g. Munteanu et al., 2021; Popescu, 1984; Rusu et al., 1983). Sandstones and shales of the Middle Miocene age with sub-horizontal structures are displayed in Figure 4 (outcrop O_3 in Figure 2, for location). Over the study area, thin layers of soil and vegetation cover the Middle-Upper Miocene formations (Figure 4).

The above information, though, is insufficient to build a subsurface structural model to the north of the Ţicău mountains.

3 | ANALYSIS AND PROCESSING OF THE AMBIENT-NOISE SEISMIC DATA

Ambient-noise seismic data were recorded along with a line with north–south orientation in the Ţicău area (the line L1 in Figure 2). Active-source seismic reflection measurements were performed

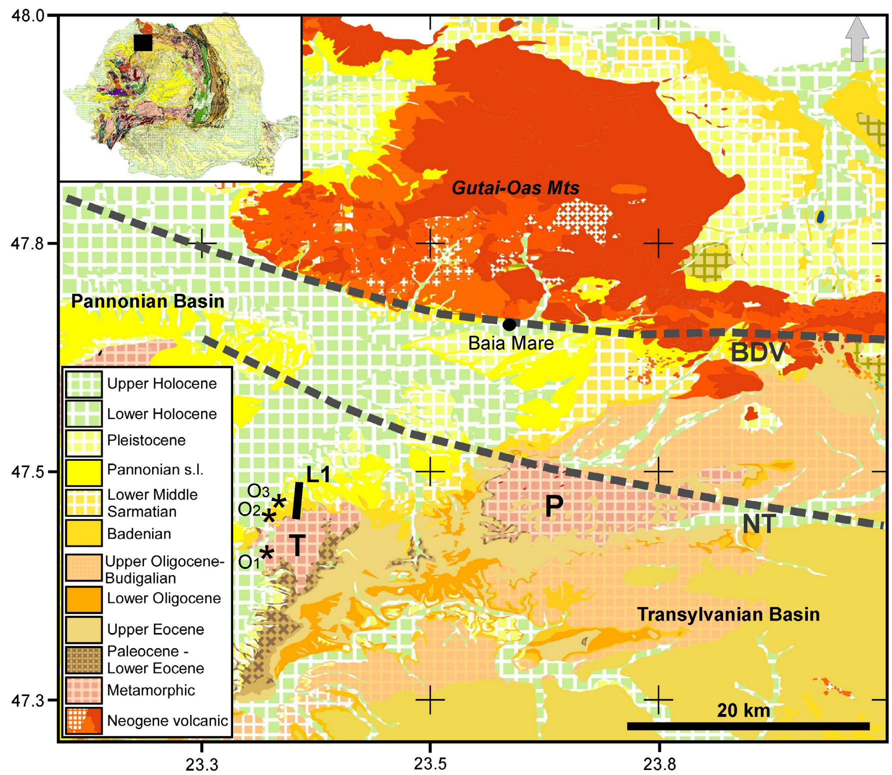

FIGURE 2 Geological map of the Ţicău area (source of the map – portal of the Geological Institute of Romania). T and P - Ţicău and Preluca crystalline islands, L1 - active-source and passive-source seismic line, BDV and NT - Bogdan-Dragoş-Vodă and North-Transylvanian faults, O_1–O_3 - outcrops shown in Figures 3 and 4. Inset: map of Romania with location of study area - black rectangle. [Colour figure can be viewed at wileyonlinelibrary.com]

along with the same line using explosive sources. The ambient-noise seismic measurements were needed as the ones based on the use of explosive sources could not be properly performed due to the field conditions. The ambient-noise and active-source data were recorded using 245 wireless receivers of 5 Hz. The receiver spacing was 12.5 m. The time sampling interval was 1 ms.

These measurements are part of a multi-disciplinary research project performed in order to investigate the structure of the Paleogene and Neogene formations developed on the north-eastern margin of the Romanian segment of the Eastern Pannonian Basin.

The ambient noise was recorded for approx. 8 h. After the recording, the data were divided and stored in panels of 10 s length. We use the SI method to retrieve body-wave reflections, considered signal during the data processing. The retrieved surface waves represent noise and will be removed from the analysed gathers. The low traffic on the national road located near the southern end of the acquisition line generated the surface waves seen on some panels.

One example of ambient-noise panel in the time domain is displayed in Figure 5. It is dominated by surface-wave arrivals generated by noise sources, which acted in the vicinity of the receiver spread. The nearly horizontal arrivals seen inside trace interval 40–80 at times 0.75–1 s might represent body-wave arrivals from relatively deeper sources. Figure 6 shows the frequency-wavenumber (f-k) amplitude spectrum of the panel in Figure 5. The spectrum shows the possible body-wave energy with apparent frequencies up to 30 Hz. The surface-wave energy is also interpreted over the same frequency interval but it is characterized by lower apparent velocities compared with the body-wave energy. The panels with strong surface waves generated by noise sources, which acted away from the acquisition line are removed after their analysis in the time and (f-k) domains.

The retrieval of body-wave reflections (e.g. Panea et al., 2014) is performed using the following steps. First, the ambient-noise panels are energy normalized per trace. Then, a master trace is chosen

FIGURE 3 Outcrops with basement formations on the southwestern part of the Ţicău mountains (O_1 and O_2 in Figure 2). [Colour figure can be viewed at wileyonlinelibrary.com]

FIGURE 4 Sandstones and shales of the Middle Miocene age (O_3 in Figure 2) on the north-western part of the Ţicău mountains covered (left) or not (right) by soil and vegetation. [Colour figure can be viewed at wileyonlinelibrary.com]

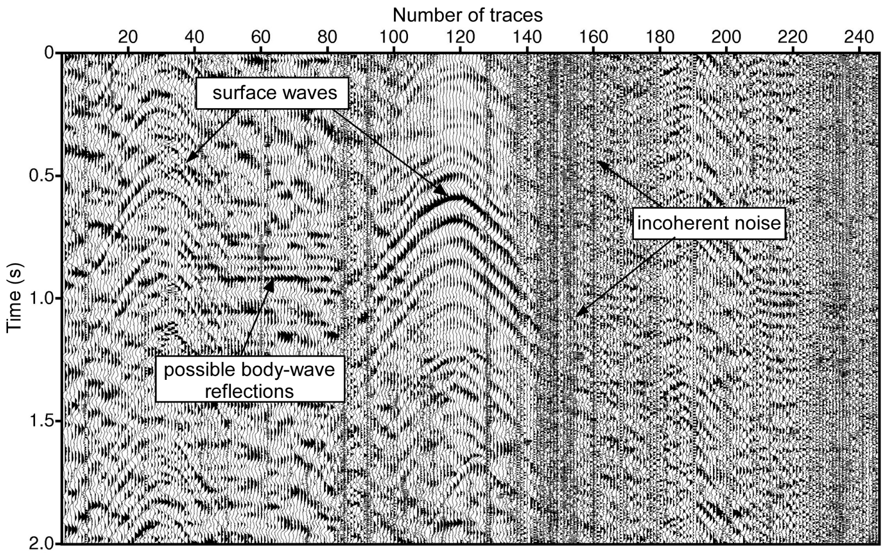

FIGURE 5 Noise panel displayed in the time domain showing possible body-wave reflections, surface waves generated by noise sources and incoherent noise.

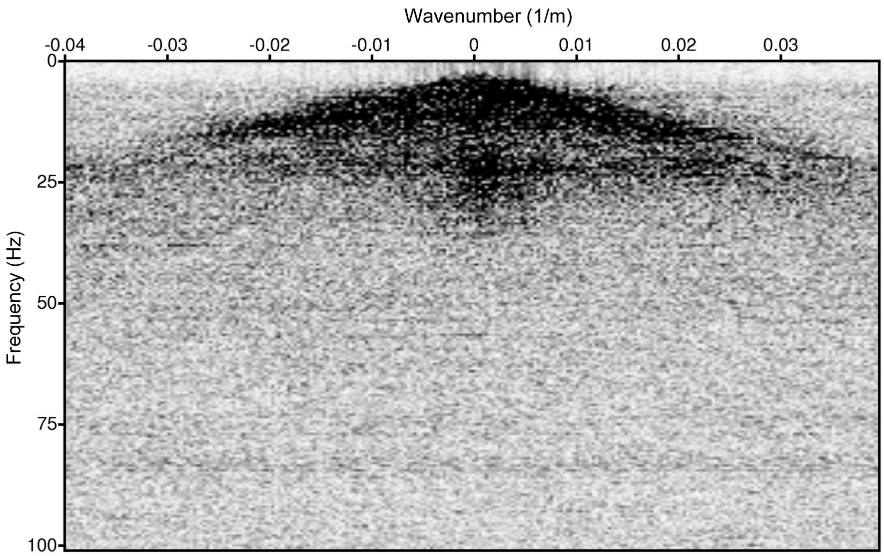

FIGURE 6 The (f, k)-amplitude spectrum of the noise panel from Figure 5.

at the location from which we want to obtain a virtual source. The spacing between the master traces is about 100 m, equal to the desired, but not fulfilled, spacing between the shot points from the active-source seismic reflection measurements. The obstacles met in the field along with the active-source seismic line forced us to modify the spacing between the points in which we generated the seismic energy using explosives.

The master trace from an ambient-noise panel is correlated with itself and with the rest of the traces of the same panel to obtain a correlated panel. For a master trace with the same receiver number, the correlation is repeated for all noise panels and the resulting correlated panels are summed together. The procedure is repeated for all master-trace locations.

The result after SI by cross-correlation response consists of 30 summed correlated panels, each panel having 245 traces. The final virtual common-source gathers are obtained by horizontally concatenating parts of the panels only at causal times and parts only at acausal times.

4 | PROCESSING OF VIRTUAL AND ACTIVE-SOURCE SEISMIC DATA

One example of virtual common-source gathering is displayed in Figure 7. It contains body-wave reflections and surface waves. The linear event interpreted above the retrieved reflections might be a virtual refraction, which propagates with the velocity from the Paleogene deposits (VR in Figure 7). The overlain Middle Miocene sedimentary deposits have thickness of tens of meters. Because of this, the shallow reflected waves might interfere with the head waves.

The nearest active-source gather to the virtual gather from Figure 7 has the shot point outside the acquisition line, near receiver

115 (Figure 8). It is dominated by surface waves. Pieces of reflected waves are seen at travel times up to 0.5 s. The active-source seismic records are characterized by low signal-to-noise ratio. The very irregular geometry used in the field for measurements affected the quality of seismic reflection data. The obstacles met along with the seismic line forced us to generate the seismic energy in points spaced at several hundreds of meters instead of approx. 100 m, as it was designed.

The virtual and active-source gathers are processed using the same flow, to allow a fair comparison of seismic sections (Figure 9a,b). We use a standard flow containing linear geometry, static corrections, frequency filtering, amplitude corrections, velocity analysis, normal move-out corrections, stacking, migration and time-to-depth conversion. The final datum of both seismic sections starts from an elevation of 300 m.

5 | DATA INTERPRETATION AND DISCUSSIONS

The passive seismic section displays folded and faulted structures along with the seismic line imaged by reflections characterized by strong amplitudes (Figure 9a). The obtained active-source seismic section looks noisy, without interpretable reflections (Figure 9b). The interpretation of the passive seismic section is done using information from existent literature, geological maps at scales 1:50,000 and 1:200,000 (e.g. Ciulavu et al., 2002; Merten et al., 2011; Popescu, 1984; Rusu et al., 1983). The first layer corresponds to the formations of Middle Miocene age (Figure 10); it appears continuous along with the line with little deformations. It is difficult to image its structure in detail because the thickness of the strata is at or even below the seismic resolution. The outcrop found in the vicinity of the

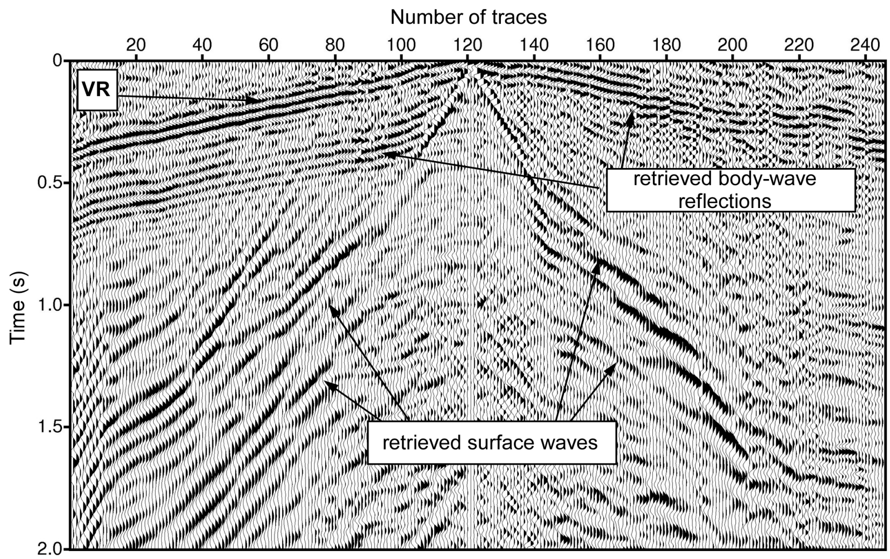

FIGURE 7 Virtual common-source gather with retrieved body-wave reflections and surface waves; master trace at receiver number 121. Trace spacing of 12.5 m. Band-pass frequency filter (2–32 Hz) applied for better display.

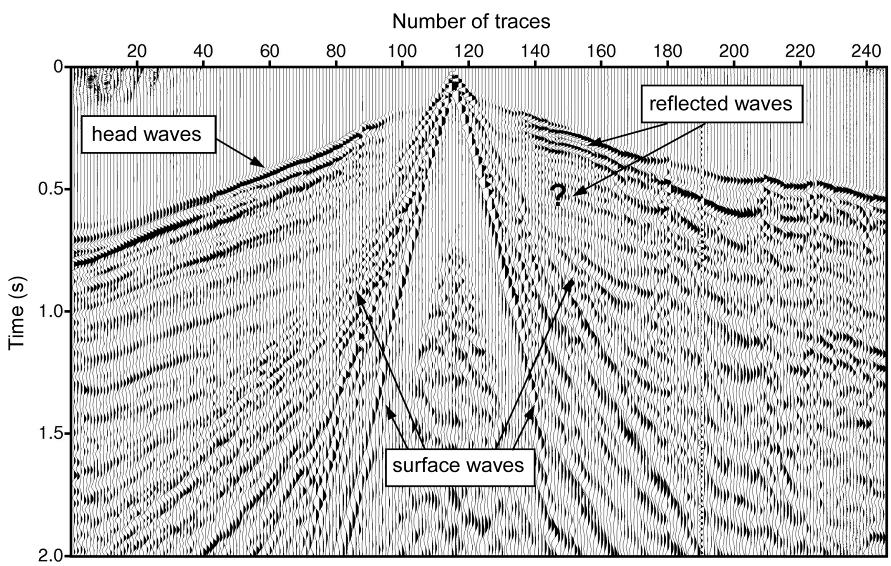

FIGURE 8 Active-source seismic reflection record with shot point near receiver number 115. Trace spacing of 12.5 m. Band-pass frequency filter (2–32 Hz) applied for better display. Static corrections have not been applied.

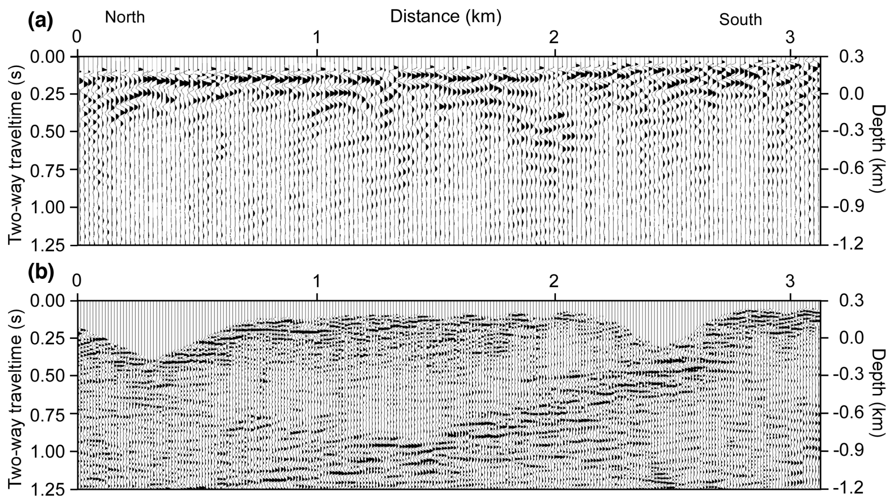

FIGURE 9 (a) Passive seismic section obtained after the processing of virtual common-source gathers. (b) Active-source seismic section obtained after the processing of seismic reflection data.

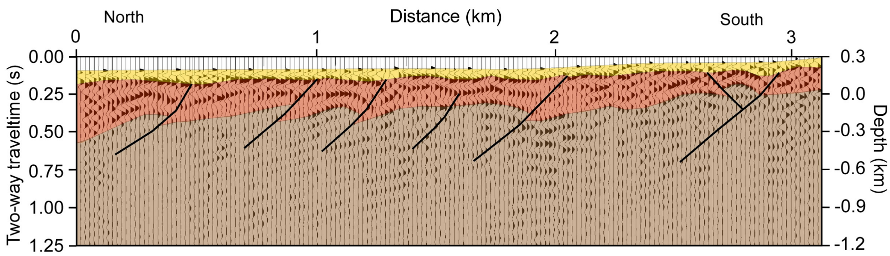

FIGURE 10 Interpreted version of the passive seismic section from Figure 9a; Middle Miocene -yellow, Paleogene - dark red and Basement - brown, possible Miocene faults – black lines. [Colour figure can be viewed at wileyonlinelibrary.com]

line provided us with information about this formation (O_3 in Figure 4). Beneath this layer, the Paleogene deposits are affected by Miocene thrust and reverse faulting and N-S folding (Figure 10). The Paleogene is represented by Palaeocene and Oligocene. Our interpretation correlates well with the observations on outcrops found on the southern part of the Ţicău mountains. The absence of Eocene and Lower Miocene (Burdigalian) deposits was documented by geological observations in the surrounding areas and by a well drilled about 25 km northeast to our study area. Their absence might be a response of the compressional movements and erosion from Eocene and of the movements along with the North-Transylvanian fault from Burdigalian (e.g. Ciulavu et al., 2002; Săndulescu, 1984). The interpreted basement appears clean. The presence of strongly deformed metamorphic rocks is responsible for the attenuation of seismic waves.

6 | CONCLUSIONS

Definition of the geological models, which explain the tectonic evolution of an area depends mainly on information obtained from geological mapping of outcrops correlated with results from geophysical measurements (e.g. active-source seismic reflection measurements). If this type of information is not available or accurate, alternative methods of subsurface investigation have to be used. In our study area, we recorded ambient-noise and active-source seismic reflection data along with the same line. The active-source seismic data are dominated by noise. The seismic section is clean, without interpretable reflections. We used seismic interferometry by cross-correlation to retrieve body-wave reflections from the recorded noise. The passive seismic section obtained after their processing displays folded and faulted reflectors interpreted to be from the Paleogene formations. Our structural image correlates well with the structural and kinematic models defined for the Paleogene-Neogene formations developed on the southern part of the Ţicău mountains, models based only on geological observations and measurements.

ACKNOWLEDGEMENTS

The authors thank the associate editor and anonymous reviewers for their constructive comments and suggestions that improved the quality of the paper. The research leading to these results has received funding from the Norway Grants 2014–2021, under Project Contract no. 12/2020. The active-source and passive-source seismic data were recorded with the help of PROSPECTIUNI S.A., Romania. Special thanks to Marius Milea, Jean Gorie, Cosmin Funieru and to all persons involved in the seismic data acquisition. The maps displayed in Figures 1 and 2 have been produced using QGIS software. The figures representing seismic data have been produced using Seismic Unix.

DATA AVAILABILITY STATEMENT

The data that support the findings of this study are available from the corresponding author upon reasonable request.

REFERENCES

Balázs, A., Matenco, L., Magyar, I., Horváth, F., & Cloetingh, S. (2016). The link between tectonics and sedimentation in back-arc basins:

New genetic constraints from the analysis of the Pannonian Basin. *Tectonics*, *35*, 1526–1559. https://doi.org/10.1002/2015TC004109
Balla, Z. (1987). Tertiary palaeomagnetic data for the Carpatho-Pannonian region in the light of Miocene rotation kinematics. *Tectonophysics*, *139*, 67–98.
Ciulavu, D., Dinu, C., & Cloetingh, S. A. P. L. (2002). Late Cenozoic tectonic evolution of the Transylvanian basin and northeastern part of the Pannonian basin: Constraints from seismic profiling and numerical modelling. *Stephan Mueller Special Publication Series*, *3*, 105–120.
Claerbout, J. (1968). Synthesis of a layered medium from its acoustic transmission response. *Geophysics*, *33*, 264–269. https://doi.org/10.1190/1.1439927
Csontos, L. (1995). Tertiary tectonic evolution of the intra-Carpathian area. A review. *Acta Vulcanologica*, *7*, 1–13.
Draganov, D., Campman, X., Thorbecke, J., Verdel, A., & Wapenaar, K. (2009). Reflection images from ambient seismic noise. *Geophysics*, *74*(5), A63–A67.
Hohl, D., & Mateeva, A. (2006). Passive seismic reflectivity imaging with ocean-bottom cable data, 76th annual international meeting, SEG, Expanded Abstracts, 1560–1564.
Horváth, F., Musitz, B., Balázs, A., Vegh, A., Uhrin, A., & Nador, A. (2015). Evolution of the Pannonian basin and its geothermal resources. *Geothermics*, *53*, 328–352. https://doi.org/10.1016/j.geothermics.2014.07.009
Kalmár, D., Hetényi, G., Balázs, A., Bondár, I., & AlpArray Working Group. (2021). Crustal thinning from orogeny to back-arc basin: The structure of the Pannonian Basin region revealed by P-to-S converted seismic waves. *Journal of Geophysical Research*, *Solid Earth*, *126*, e2020JB021309. https://doi.org/10.1029/2020JB021309
Márton, E., & Fodor, L. (2003). Tertiary paleomagnetic results and structural analysis from the Transdanube range (Hungary): Rotational disintegration of the AlCaPa unit. *Tectonophysics*, *363*(3–4), 201–224.
Merten, S., Matenco, L., Foeken, J. P. T., & Andriessen, P. A. M. (2011). Toward understanding the post-collisional evolution of an orogeny influenced by convergence at adjacent plate margins: Late cretaceous-tertiary thermotectonic history of the Apuseni Mountains. *Tectonics*, *30*, TC6008. https://doi.org/10.1029/2011TC002887
Munteanu, I., Panea, I., & Roban, R. (2021). Structure of the north eastern Pannonian Basin, Romania, a Review, Conference Proceedings, 11th Congress of the Balkan Geophysical Society, Volume 2021, 1–5.
Panea, I., Draganov, D., Almagro-Vidal, C., & Mocanu, V. (2014). Retrieval of reflections from ambient noise recorded in the Mizil area, Romania. *Geophysics*, *79*(3), Q31–Q42.
Popescu, B. M. (1984). Lithostratigraphy of cyclic continental to marine Eocene deposits in NW Transylvania, Romania. *Comptes Rendu Des Sceances*, *Societe de Physique Et d'hystoire Naturelle de Geneve*, *37*, 37–73.
Răbăgia, A. M. (2009). Studies of sequential stratigraphy in the northern part of the Pannonian Basin to establish its tectonic and stratigraphic evolution, doctoral dissertation, University of Bucharest, in Romanian, 111 pp.
Reiser, M. K., Săbău, G., Negulescu, E., Schuster, R., Tropper, P., & Fügenschuh, B. (2019). Post-variscan metamorphism in the Apuseni and Rodna Mountains (Romania): Evidence from Sm-Nd garnet and U-Th-Pb monazite dating. *Swiss Journal of Geosciences*, *112*, 101–120.
Ruigrok, E., Campman, X., & Wapenaar, K. (2011). Extraction of P-wave reflections from microseisms. *Comptes Rendus Geoscience*, *343*, 512–525. https://doi.org/10.1016/j.crte.2011.02.006
Rusu, A., Balintoni, I., Bombita, G., & Popescu, G. (1983). Geological map of Romania, Preluca Map, Geological Institute of Romania, Scale 1:50000.
Sabra, K. G., Gerstoft, P., Roux, P., Kuperman, W. A., & Fehler, M. C. (2005). Extracting time-domain Green's function estimates from ambient seismic noise. *Geophysical Research Letters*, *32*, L03310. https://doi.org/10.1029/2005GL023155
Săndulescu, M. (1984). Geotectonica României. Ed. Tehnică, Bucureşti, in Romanian.
Săndulescu, M. (1988). Cenozoic tectonic history of the Carpathians. *AAPG Memoir*, *45*, 17–25.
Schmid, S. M., Bernoulli, D., Fügenschuh, B., Matenco, L., Schefer, S., Schuster, R., Tischler, M., & Ustaszewski, K. (2008). The Alpine-Carpathian-Dinaridic orogenic system: Correlation and evolution of tectonic units. *Swiss Journal of Geosciences*, *101*, 139–183. https://doi.org/10.1007/s00015-008-1247-3
Schmid, S. M., Fügenschuh, B., Kissling, E., & Schuster, R. (2004). Tectonic map and overall architecture of the Alpine orogeny. *Eclogae Geologicae Helvetiae*, *97*, 92–117.
Schmid, S. M., Fügenschuh, B., Kounov, A., Matenco, L., Nievergelt, P., Oberhänsli, R., Pleuger, J., Schefer, S., Schuster, R., Tomljenović, B., Ustaszewski, K., & van Hinsbergen, D. J. J. (2020). Tectonic units of the Alpine collision zone between eastern Alps and western Turkey. *Gondwana Research*, *78*, 308–374.
Shapiro, N. M., & Campillo, M. (2004). Emergence of broadband Rayleigh waves from correlations of the ambient seismic noise. *Geophysical Research Letters*, *31*, L07614. https://doi.org/10.1029/2004GL019491
van Manen, D.-J., Robertson, J. O. A., & Curtis, A. (2005). Modeling of wave propagation in inhomogeneous media. *Physical Review Letters*, *94*, 164301. https://doi.org/10.1103/PhysRevLett.94.164301
Wapenaar, C. P. A., Thorbecke, J., Draganov, D., & Fokkema, J.T., 2002. Theory of acoustic daylight imaging revisited, 72nd Annual International Meeting, SEG, Expanded Abstracts, 2269–2272.
Wapenaar, K., & Fokkema, J. (2006). Green's function representations for seismic interferometry. *Geophysics*, *71*(4), SI33–SI46. https://doi.org/10.1190/1.2213955
Xu, Z., Juhlin, C., Gudmunsson, O., Zhang, F., Yang, C., Kashubin, A., & Luth, S. (2012). Reconstruction of subsurface structure from ambient seismic noise: An example from Letzin, Germany. *Geophysical Journal International*, *189*, 1085–1102.
Zhan, Z., Sidao, N., Helmberger, D. V., & Clayton, R. W. (2010). Retrieval of moho-reflected shear wave arrivals from ambient seismic noise. *Geophysical Journal International*, *182*, 408–420. https://doi.org/10.1111/j.1365-246X.2020.04625x

How to cite this article: Panea, I., Draganov, D., Bouaru, C. F., & Munteanu, I. (2023). Imaging of post-collisional deformations on the NE Tisza continental unit using ambient seismic noise: A case study from the Ţicău area, Romania. *Terra Nova*, *35*, 432–439. https://doi.org/10.1111/ter.12667